Computational modelling of ray propagation through optical elements using the principles of geometric optics

Son-Gyo Jung
Department of Physics, Imperial College London
CID: 00948246
Group A9
(Dated: February 5, 2016)

By applying the principles of geometric optics, imaging performances of lenses were investigated via examining the propagation of optical rays through various optical systems. The optical system and its elements were modelled with an object-oriented approach using the Python programming language. Through utilising a ray bundle with specific parameters, the performances of a planoconvex lens with different orientations were analysed. The orientation with the convex surface facing the incident beam was found to be more effective at minimising the spherical aberration. This was evident from the value of the geometric RMS spot radius of 1.85×10^{-5}m at the paraxial focus compared to 7.04×10^{-5}m for the plano-convex orientation. This was further supported by the relatively slow rate of increase in the RMS spot radius with the beam size for the convex-plano orientation. Furthermore, by optimising the curvatures of a singlet lens with a image distance of 100mm, the best form curvatures were approximated as 0.01417mm^{-1} and -0.00532mm^{-1} with the RMS spot radius of 6.07×10^{-8}m, leading to a conclusion that the system was diffraction limited and the effect of diffraction was substantial when using a beam radius smaller than 13.60mm.

1. Introduction

In this investigation, the behaviour of optical rays through different types of transmissive optical elements which refract incident light beams were computationally analysed. A model of optical ray tracing system comprising a simple, transparent glass lens was constructed using the Python programming language. The simulations involved propagating a bundle of rays through an optical element and examining its performance by determining the paraxial focus and subsequently the geometric Root-Mean-Square (RMS) spot radius. Using these results, the limitations of certain lens orientations were studied with a final intention to optimise the performance of a biconvex lens, a singlet with two spherical surfaces, for a given output plane. This was accomplished by calculating the optimal curvatures for each spherical surface whilst reducing the deviation of the focal spot size from the optical axis and thus minimising the effect of spherical aberration.

This report comprises the theoretical framework that supports the investigations, an outline of the method and the set up of each investigation, a detailed analysis of the results and the summary of the findings with concluding statements.

2. Theory

2.1 Snell's Law of Refraction

When waves are incident on an interface between two different dielectric media, they experience changes in their velocities and consequently in their direction of propagation - they are said to have undergone refraction. By examining this phenomenon, which is consistent with the wave equation in the limit of the wavelength becoming infinitesimal, properties of both media can be determined very accurately. Refraction is incorporated into the model of the optical system by using Snell's law given by the equation:

$$\eta_1 sin\theta_1 = \eta_2 sin\theta_2, \tag{1}$$

where η_1 and η_2 are the refractive indices of the first and second media respectively, θ_1 is the angle of incidence and θ_2 is the angle of refraction.[1]

When waves are incident upon a less dense medium, there is an angle beyond which no waves are transmitted but undergo total internal reflection. This angle is known as the critical angle. Critical angle is dependent on the refractive indices of the two media. In fact, it is the inverse sine of the ratio between the second and the first refractive indices.

The key assumption that is made while applying Snell's law is that the media are isotropic; that is, assuming both media are uniform in composition in all directions. In addition to Equation (1), the vector form of Snell's law was critical in modelling the behaviour of the transmitted optical rays through each refracting surface. This is given by:

$$\mathbf{t} = \frac{\eta_1}{\eta_2}\hat{\mathbf{k}} + (\frac{\eta_1}{\eta_2} cos\theta_1 - \sqrt{1 - sin^2\theta_2})\hat{\mathbf{n}}, \tag{2}$$

where $sin^2\theta_2 = (\frac{\eta_1}{\eta_2})^2(1 - cos^2\theta_1)$, $\mathbf{t}$ is the refracted direction vector, $\hat{\mathbf{k}}$ is the unit vector in the direction of the ray and $\hat{\mathbf{n}}$ is the unit vector normal to the refracting surface.[2]

2.2 Spherical Aberration

In an ideal case, optical rays refracting through a spherical lens can be made to converge at a single point known as the focal point. However, in practice, rays fail to converge at a single point and a blurring effect occurs. This

optical effect, known as the spherical aberration, is a result of the rays propagating parallel to the optical axis through a spherical lens at different distances from the axis.[1,3] The rays further away from the optical axis experience greater refraction and thus they intersect the optical axis slightly behind the paraxial focus before diverging (FIG. 1).

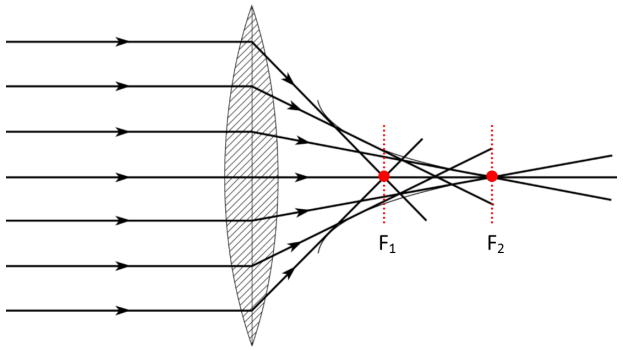

FIG. 1: A lens displaying spherical aberration; the marginal and paraxial rays focus at the points F_1 and F_2 respectively.[3]

For a single lens, spherical aberration can be minimised either by changing the orientation of the lens or by carefully choosing the curvatures of the spherical surfaces into the best form. In this investigation, both cases are examined using collimated ray bundles with uniformly distributed rays of various diameters with the aim to minimise this effect.

2.3 Geometric RMS Spot Radius & Diffraction limit

To quantitatively analyse the effect of spherical aberration, the size of the geometrical focus can be calculated by computing the deviation of the rays in the focal plane from the optical axis; this is equivalent to the RMS spot radius at the paraxial focus for a given ray bundle.[1] Therefore, by minimising the RMS spot radius, the spherical aberration is likewise minimised. In the latter part of the investigation, the optimal curvatures of the spherical surfaces are determined by utilising this approach.

However, in addition to the geometric RMS spot radius, the resolution of an optical imaging system can be limited by other factors. One such factor that fundamentally limits the maximum resolution of any optical system is diffraction.[1,4] Therefore, when using a lens that is diffraction limited, the presence of any deviation at the paraxial focus is attributed to the effect of diffraction of rays rather than the effect of spherical aberration. It is thus essential to take diffraction scale into consideration. The diffraction limit, d, is given by the equation:

$$d = \frac{\lambda f}{D}, \tag{3}$$

where λ is the wavelength of the light, f is the focal length and D is the diameter of the input beam.[1] Using Equation (3), the comparison between the RMS spot radius and the diffraction limit can be made in order to determine the nature of the aberration observed in an optical system.

3. Methods

3.1 Modelling a Single Spherical Surface

An initial testing was carried out by modelling a simple system consisting of a single spherical refracting surface with a curvature of 0.03mm^{-1}. The system was set up so that the optical axis was along the z-axis and the values of the refractive indices of the two media, η_1 and η_w, were set as 1.0 and 1.5, respectively. With the refracting surface and the output plane placed at $z = 100$mm and $z = 250$mm respectively, the paraxial focus was calculated by propagating a paraxial ray through the lens. Following this, the position of the output plane was adjusted to the paraxial focus and a collimated beam with a diameter of 10mm was used to estimate the size of the geometrical focus. The estimation was made by computing the RMS deviation of the individual ray positions from the optical axis on the output plane.

3.2 Modelling a Planoconvex Lens

A more practical investigation was carried out by modelling a lens with two refracting surfaces, namely the planoconvex lens. Planoconvex lens was constructed with a planar element and a convex element with a curvature of 0.02mm^{-1} separated by a distance of 5mm. The refractive index of the optical element was adjusted to 1.5168 in order to accurately approximate the air-glass boundary, and the wavelength of the light beam was assumed to be 588nm. Subsequently, the performance of the lens in focusing a collimated light with a uniform distribution of rays and a beam diameter of 10mm was studied using two different orientations: plano-convex and convex-plano.

In each case, the paraxial focus was calculated using a paraxial ray as with the single spherical refracting surface. The RMS deviation from the optical axis on the output plane was then calculated as a measure of the geometrical spot size. This process was repeated using bundles of rays of radii ranging from 1mm to 10mm in order to examine the relationship between the RMS spot radius and the beam radius.

3.3 Lens optimisation

Ultimately, a singlet with two spherical refracting surfaces was designed with the curvatures carefully chosen to optimise its performance for a given object and image distance. This was achieved by using an optimiser function that minimised the RMS deviation from the optical axis at a given output position at $z = 202.5$mm (a focal length of 100mm) with a ray bundle of 5mm radius. This process was repeated using ray bundles of radii ranging from 1mm to 20mm to generate a plot illustrating the behaviour of the RMS spot radius and the diffraction limit with the beam size.

Eventually, quantitative and qualitative comparisons of the results from this simulation and those obtained for the planoconvex lens were made.

Note: see the lab book p.108-20, 132 for the systematic methodology adopted in modelling the optical system.

4. Results and Discussion

For the system comprising of a single refracting surface with a curvature of 0.03mm^{-1} positioned at $z = 100\text{mm}$, the RMS spot radius was calculated as $4.79 \times 10^{-5}\text{m}$ at the paraxial focus at $z = 200\text{mm}$. This corresponds to a focal length of 100mm, which is consistent with the value calculated using the principle of geometric optic in the limit of small angle (see lab book (LB) p.124 for the calculation), suggesting the model of the optical ray tracing system is operative. Further evidence of the working model is demonstrated in Fig. 2. Moreover, the diffraction limit was calculated as 5.88×10^{-6}, implying that the system was not diffraction limited. Hence, the deviation of the rays at the paraxial focus was concluded to be a result of spherical aberration (see LB p.122-3 for the full results).

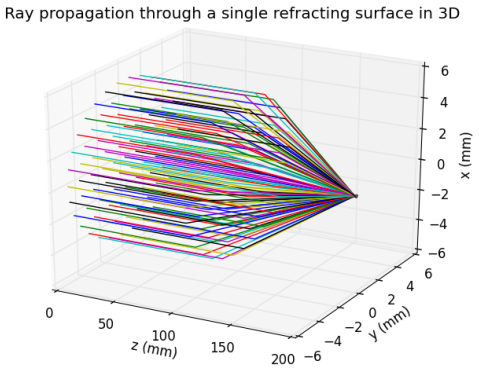

FIG. 2: A ray bundle of radius 5mm propagating through a single spherical surface with a curvature of 0.03mm^{-1} and refracting towards the optical axis.

With the system modelling a planoconvex lens with a curvature of 0.02mm^{-1} for the convex surface, the RMS spot radius was calculated as $7.04 \times 10^{-5}\text{m}$ at the paraxial focus located at $z = 201.75\text{mm}$ for the planoconvex orientation. This corresponds to a focal length of 99.25mm and a diffraction limit of $5.84 \times 10^{-6}\text{m}$. With the convex-plano orientation, the simulation estimated the RMS spot radius as $1.85 \times 10^{-5}\text{m}$ at the paraxial focus located at 198.45mm, thereby yielding a focal length of 95.95mm and a diffraction limit of $5.64 \times 10^{-6}\text{m}$. These results indicate that the effects of spherical aberration were present for both orientations and any effect caused by diffraction was minuscule. However, the orientation where the convex surface was facing the input was noticeably more effective at minimising the RMS spot radius with a relative difference of 1.17; that is a percentage difference of 117%. The difference in the degree of spherical aberration is visually illustrated in FIG. 3.

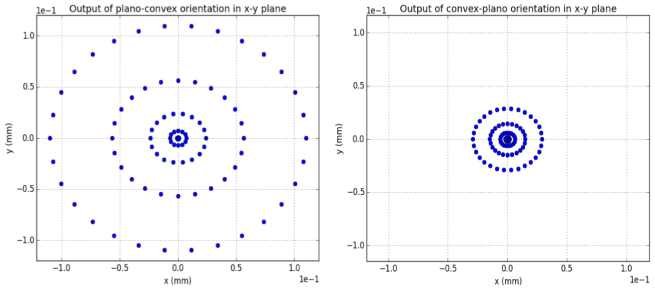

FIG. 3: The non-uniform ring pattern that is shown in the figure is symbolic of the spherical aberration effect. The aberration is significantly reduced using the convex-plano orientation.

The last investigation using the planoconvex model was to examine the variation of RMS spot radius with the radius of the beam. FIG. 4 below shows that the RMS spot radius at the paraxial focus for both orientations increases as the beam radius gets larger. The rate at which the RMS spot radius increases was found to be consistently greater with the plano-convex orientation, which is in line with the initial indication. The difference in the performances is in agreement with the principles of geometric optics. The input rays propagating parallel to the optical axis do not refract as they intersect the plane surface. Thus the direction of propagation changes only at the convex surface, reducing the amount of refraction that is possible when compared to the convex-plano orientation. This effect becomes significant as the distance of the input rays from the optical axis increases. As a result, the rays converge slightly behind the paraxial focus and consequently the RMS spot radius at the paraxial focus grows with the radius of the ray bundle.

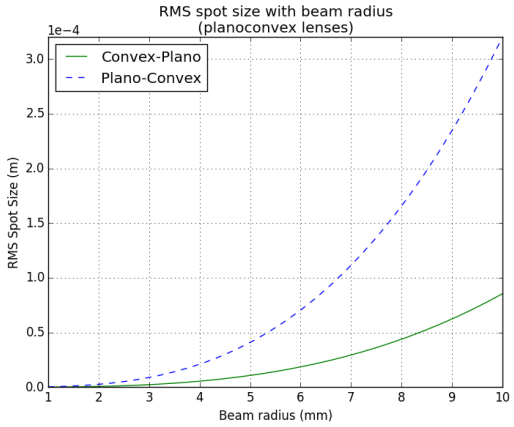

FIG. 4: A graph depicting the change in the RMS spot radius at the paraxial focus with increasing beam size.

The optimisation of the singlet lens using a 5mm beam radius and a focal length of 100mm yielded the best

form lens curvatures as 0.01417mm^{-1} and -0.00532mm^{-1} for the first and second lens respectively. The resulting model of the biconvex lens gave the RMS spot radius as 6.07×10^{-8}m with the diffraction limit of 5.88×10^{-6}m, confirming that the system was diffraction limited. The improvement of the performance of the lens is comparatively significant to the plano-convex model as the effect of spherical aberration was completely minimised for the given focal length of 100mm. The major limitation of the imaging performance was therefore no longer due to spherical aberration but was fundamentally restricted by the effect of diffraction.

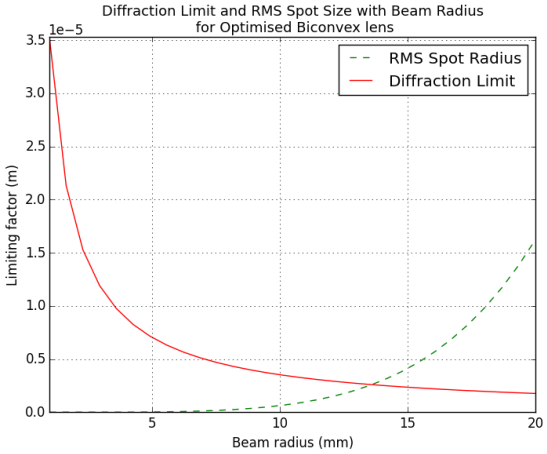

FIG. 5: A graph showing the relationships of the diffraction limit and the RMS spot radius with increasing beam size.

FIG. 5 shows that the optical system consisting of the optimised biconvex lens became diffraction limited below the beam radius of 13.60mm, which corresponds to the point of intersection of the two curves. The figure further illustrates that the diffraction limit rises extremely rapidly in the limit of small radius. This observation is noticeable below the radius of 5mm. In general, this pattern is observed for all optical systems and for this reason there is a restriction on the maximum resolution that an optical system can achieve.

4. Conclusion

To summarise, the computational modelling of the optical ray tracing system using the principles of geometric optics verified the physical observation of spherical aberration and also provided an insight of diffraction limited optical systems.

In the model, the rays propagating through an optical element was found to deviate from the ideal (paraxial) behaviour as the distance of the input ray from the optical axis was increased. Subsequently, the planoconvex lens with the convex surface facing the incident beam was found to be more effective at minimising spherical aberration with the RMS spot radius of 7.04×10^{-5}m. In this particular simulation with a beam radius of 5mm, the percentage difference between the values of the RMS spot radius at the paraxial focus for the two orientations was calculated to be 117%. The RMS spot radius was found to increase with the growing beam radius for both orientation. Nevertheless, the convex-plano orientation was shown to be less affected by spherical aberration.

Through optimising a singlet lens with a focal length of 100mm, the resulting biconvex lens with curvatures of 0.01417mm^{-1} and -0.00532mm^{-1} for the first and second lens was found to produce the least overall aberration. Moreover, the comparison between the diffraction limit and the RMS spot radius with increasing beam radius suggested that any optical system are fundamentally limited by diffraction whilst this particular model was diffraction limited below the beam radius of 13.60mm.

Possible improvement includes adjusting the model in order to simulate the dependence of the refraction angle on the frequency of an incident light, which is cause by the material dispersion. In this case, the refractive indices of the media could be modelled so that the values depend on the frequencies of the incident rays, allowing more naturalistic observations to be simulated.

[1] C. Paterson, *An Optical Ray Tracer*, Department of Physics, Imperial College London, Oct 2015, [Online] Available at: https://bb.imperial.ac.uk/bbcswebdav/pid-698942-dt-content-rid-25269551/courses/COURSE-PHY2LAB-1516/Y2Computing/Y2PyCourse/Students/Projects/Raytrace [04.02.16]

[2] Bram de Greve, *Reflections and Refractions in Ray Tracing*, Stanford University, Nov. 2006, [Online] Available at: http://graphics.stanford.edu/courses/docs/2006-reflectionrefraction [25.01.16]

[3] G. J. Robinson, *Optical instruments*, University of Reading, The Open University, 1996, [Online] Available at: http://www.met.reading.ac.uk/pplato2/h-flap/phys64 [25.01.16]

[4] E. Rogers, N. Zheludev, *Beating the diffraction limit with super-oscillations*, Journal of Optics, IOP, 2013, [Online] Available at: http://iopscience.iop.org/2040-8986/labtalk-article/55022 [25.01.16]